

DesignCon 2006

Theory and Measurement of Unbalanced Differential-Mode Transmission Lines

Stephen B. Smith, FCI USA, Inc.

stephen.smith@fciconnect.com

Sedig S. Agili, Penn State University.

ssa10@psu.edu

Vittal Balasubramanian, FCI USA, Inc.

vittal.balasubramanian@fciconnect.com

Abstract

When characterizing a differential-mode transmission path, it is usually assumed that the differential pair is balanced thereby simplifying the analysis. The theory and characterization of balanced pairs is well-established. By contrast, the theory of unbalanced differential pairs has not been extensively investigated despite the fact that such pairs appear in many applications.

A complete generic model and characterization of unbalanced differential transmission line pairs is presented. Pairs having geometrical or impedance imbalance as well as pairs having temporal imbalance (also known as in-pair skew) are considered. The paper also describes how to accurately characterize unbalanced lines using TDR and VNA measurements.

Authors' Biographies

Stephen B. Smith's current responsibilities include the design and analysis of high-speed connectors. He also engages in customer support activities working very closely with Marketing and Sales. Prior to coming to FCI in 2000, Smith worked at AMP Incorporated (now Tyco Electronics) for 10 years as a development engineer spending most of that time in the electromagnetics research group where he developed methods of modeling and simulating interconnection systems on projects spanning the frequency spectrum from power-frequency high-current utility connectors to high-speed and r.f. interconnects. Prior to that, he worked in acoustical research at Masland Industries (now Lear Corporation.) He has taught various courses at each of his jobs, and in the last couple of years, he has presented papers at the 2003 Conference on Information Science and Systems at The Johns Hopkins University and at the IEEE Holm Conference. At last year's DesignCon West, he acted on behalf of the entire design team when he accepted the first annual DesignVision Award for the AirMax VS® Connector System. Smith has a B.S. in physics and an M.S.E.E., both from Penn State University.

Sedig S. Agili received his BS, MS, and Ph.D. in Electrical and Computer Engineering from Marquette University in 1986, 1989, and 1996, respectively. As a student, he was awarded fellowships from Marquette University and the U.S. Department of Education. Upon receiving his Ph.D., he joined the faculty at Marquette University where he taught several courses in electrical engineering and conducted research in the area of electro-optic devices, fiber optic communication and fiber optic sensors. In fall of 2001, he joined the electrical engineering and electrical engineering technology programs at Penn State University, Capital College. Currently he is teaching and conducting research in electronic communications, fiber optic communications, fiber optic sensors and signal processing. He has authored several articles published in journals and conference proceedings, and made presentations at many conferences and seminars. He also worked for Astronaut Corporation of America in Milwaukee, Wisconsin where he was involved in designing optical projection and heads-up display systems. He is a member of the Institute of Electrical and Electronic Engineers, American Society for Engineering Education, and Sigma Xi.

Vittal Balasubramanian received his BS in Electrical Engineering from Delhi College of Engineering, University of Delhi in 2001. He is currently pursuing his MS in Electrical Engineering at Penn State University since spring 2003. At Penn State, he was awarded the Doris Hughes Memorial Award which recognizes international students for outstanding academic achievement and contribution to the college community. Prior to starting his MS at Penn State, he worked at Sapien Corporation Pvt. Ltd., from August 2001 to December 2002. He is currently working at FCI USA, Inc. where his responsibilities include the design and analysis of high-speed connectors. He is a member of the Institute of Electrical and Electronics Engineers since 1998.

1. Introduction

In the early days of computers, a stream of data was transmitted on a single transmission line serially. This worked very well for the computers of yesterday with speeds barely reaching a few hundred Mbits/s. With the development of new transceiver devices which could transmit data at much higher speeds, it became necessary to introduce transmission lines which could transport the data just as fast. Increasing speeds pushed the limits of communication/data transmission over a single transmission line comprised of a signal and ground conductor (generally known as single-ended transmission.) In the current market, high speed transmission with data rates typically greater than 1 Gbits/s is becoming increasingly important for both communication and data applications. For such high speeds, signal transmission quality over a single-ended line quickly deteriorates to the unusable. For such applications, it becomes necessary to use two signal conductors in a differential-mode configuration to effectively transmit the data. In the differential signaling methodology, two signal conductors are used to transmit a single bit of information from the transmitter to the receiver [1]. Data is transmitted on the two signal conductors in tandem. As one line goes low relative to ground, the other line goes high and vice versa. Differential-mode signaling has multiple advantages over single-ended signaling [2], such as:

- The propagation of a differential signal over a differential pair is more robust to crosstalk and discontinuities,
- The propagating differential signal through a connector or package is less susceptible to switching noise,
- The differential amplifier at the receiver end can have a higher gain than a single-ended amplifier,
- The total dI/dt (instantaneous rate of change of current) from the output drivers is greatly reduced over that of single-ended drivers, lessening the chances of a rail collapse and potentially reducing EMI (Electro-Magnetic Interference), and
- A low cost, twisted-pair cable can be used to transmit a differential signal over long distances.

Despite all these advantages, there are things that one needs to consider carefully when using differential-mode signaling. There's the obvious downside that transmitting a differential signal requires twice the number of signal lines as transmitting a single-ended signal. Also, if differential signals are not properly balanced or filtered, common-mode signal will be generated, and a real differential signal driven by an external twisted-pair cable can cause EMI problems.

Given the advantages of differential-mode signaling and with the push for ever increasing data rates, it has become essential to move from single-ended signaling to differential-mode signaling. Ideally, the transmission path for a differential signal should be perfectly balanced. However, practical restrictions on the design of transmission lines for differential-mode signaling inherently introduce some level of imbalance. What this means is that new designs are built with the very real possibility of having EMI problems caused by the imbalance in the differential transmission line. The EMI problems are becoming more and more important as data rates start to push beyond 5 Gbits/s. As a result, it has become important to characterize these unbalanced coupled transmission lines.

There have been multiple attempts at characterizing coupled transmission lines which form the basis of differential-mode signaling. In [3], Cohn presented an analysis of the odd and even TEM modes on a pair of parallel co-planar strips midway between two ground planes. The author derived the characteristic impedances and phase velocities of the two modes. At the time of the paper by Cohn, the application of such a parallel co-planar pair was mainly in directional couplers, band-pass filters, delay lines, single-to-balanced strip-line transformer, etc. In [4], Zysman, et. al., obtained ABCD parameters

of a two-port network composed of two identical coupled transmission lines embedded in an inhomogeneous dielectric. Both [3] and [4] assumed the coupled lines to be balanced. In [5], Tripathi derived the terminal characteristic parameters for a uniform coupled-line four-port network for the general case of an asymmetric, inhomogeneous medium in terms of two independent modes. All these characterizations [3-5], were in terms of characteristic impedances, phase velocities, and/or ABCD parameters. However, none of these consider differential- and common-mode signaling, nor do they consider scattering parameters of the coupled transmission lines.

In [6], K. Kurokawa defined the now famous scattering matrix based on wave equations for a balanced single-ended coupled line system. Bockelman et. al. [7] presented a theory for combined differential- and common-mode normalized waves in terms of even- and odd-mode impedances and propagation constants for a coupled line. These are related to even- and odd-mode terminal currents and voltages. The authors started with an unbalanced coupled line, but then as they developed the mixed-mode S-parameters, they made a simplifying assumption whereby they assumed the unbalanced lines to be balanced. They then proceeded to develop the generalized mixed-mode S-parameters of a balanced two-port system.

As can be seen from the preceding discussion, little has been done to develop the generalized S-parameters and mixed-mode representation of an asymmetric coupled transmission line. In this paper, a theoretical model and characterization of unbalanced differential pairs is presented. Pairs having geometrical (impedance) imbalance as well as pairs having temporal imbalance (also known as skew) are considered. These pairs are characterized using impedance matrices as well as S-parameter representations. This rigorous analysis of unbalanced pairs is compared to the more common practice of treating unbalanced pairs as if they were balanced. The pairs are measured both in the time-domain using a time-domain reflectometer (TDR) as well as in the frequency domain using a vector network analyzer (VNA,) and the measurements are used to validate the models arising from theory. Based on the developed theory, it is also verified whether the TDR and the VNA measurements report the true differential impedance and S-parameters for unbalanced transmission lines, respectively.

2. Balanced differential pairs

The characterization of the modes of propagation and operation of a differential transmission line has its origin in the need to properly terminate such a line. Transmission lines must be terminated in order to reduce or eliminate unwanted signal reflections. For single-ended transmission lines, termination simply consisted of placing at each end of the transmission line, a resistor whose value was equal to that of the characteristic impedance of the transmission line. A similar approach must be taken for differential-mode lines. In practice, this usually consists of terminating both ends of each signal line with a single resistor, typically 50Ω . Despite the widespread use of this simple termination, a differential pair actually exhibits multiple TEM or quasi-TEM modes, and, in theory, each of these modes should be properly terminated as shown in Figure 1. Figure 1(a) shows a hypothetical differential-mode transmission line structure consisting of two wires over a ground plane. A cross-sectional view of one end of the conductors appears in Figure 1(b) with resistors to terminate all of the modes. The values of the resistors can be calculated from measurements of the impedance of each of the modes. In addition to this, the values of these resistors equate to the values of the impedances existing between the lines, and can be used to construct a model of the differential pair.

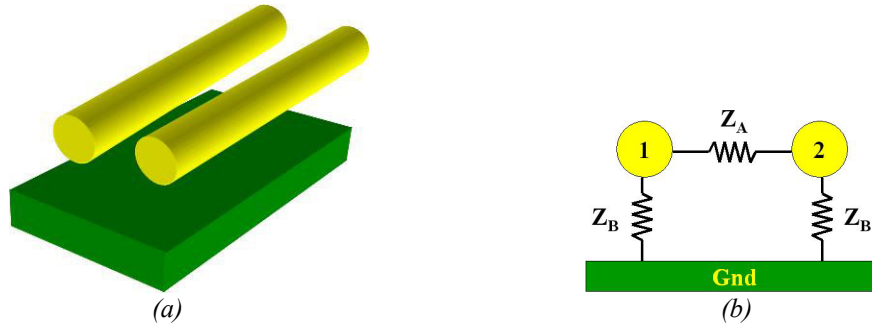


Figure 1: (a) Differential Transmission Line Consisting of Two Coupled Lines Over a Ground Plane. (b) An End View of the Line Shown in (a), With Resistors to Terminate the Modes.

The multiple TEM or quasi-TEM modes of operation of a coupled transmission line are typically characterized by their characteristic impedance and phase velocity. The quantity relating the magnitudes of the voltage and current of the traveling wave on a transmission line is designated as the impedance and has the symbol Z_0 and has the units of “ohms”. Phase velocity is generally defined as the rate at which the phase of a wave propagates along the transmission path. In the following sections, the impedance of each mode is shown first in terms of the intrinsic impedances between each line, (i.e. Z_A and Z_B), and then in terms of the per unit length inductance and capacitance values of the lines. Likewise, the phase velocities of each of the modes are shown. The terms inductance and capacitance, wherever used in this chapter shall refer to the per unit length inductance and the per unit length capacitance, respectively.

The model used to calculate the partial self and mutual inductances associated with each conductor in Figure 1(a) is shown in Figure 2(a). Because the lines are balanced, $L_{11}=L_{22}$, and $M_{1g}=M_{2g}$. Figure 2(b) shows a cross-sectional view of the conductors in Figure 1(a) with representation of the equivalent capacitance per unit length between each conductor. This is used to calculate the capacitance for each mode. Here, the balance in the lines dictates that $C_{1g}=C_{2g}$.



Figure 2: (a) Partial Self and Mutual Inductances Associated With Each Conductor in Figure 1(a). (b) Equivalent Capacitance per Unit Length Between Each Conductor in Figure 1(a).

2.1 Parameters for Balanced Lines

The following sub-sections give the impedance and phase velocity for each of the coupled-line modes in terms of the inductances and capacitances shown in Figure 2.

2.1.1 Single-Ended

Single-ended systems require just one line for each signal. There is also a second line which acts as the ground/return path for the signal current. A single-ended system also requires a global common

reference for all the signals. In a high-speed design, this reference is usually distributed throughout the system as a ground plane. The use of a shared reference for all circuits is called *single-ended signaling*.

From Figures 1(b), the single-ended impedances, Z_{SE1} and Z_{SE2} , are:

$$Z_{SE1} = Z_{SE2} = Z_B \parallel (Z_A + Z_B) = \frac{Z_B(Z_A + Z_B)}{Z_A + 2Z_B} \quad (1)$$

where, Z_A is the impedance between the two conductors and Z_B is the impedance between each conductor and ground,

The single-ended characteristic impedance, Z_{SE} , is:

$$Z_{SE} = \sqrt{\frac{L_{11} + L_{gg} - 2M_{1g}}{C_{1g} + \frac{C_{12}C_{1g}}{C_{12} + C_{1g}}}} \quad (2)$$

where C_{12} is the capacitance between conductor 1 and conductor 2, C_{1g} is the capacitance between conductor 1 and ground, and C_{2g} is the capacitance between conductor 2 and ground, and L_{11} is the partial self inductance of line 1, L_{gg} is the partial self inductance of the ground, and M_{1g} is the partial mutual inductance between line 1 and ground. Note that in equations (2) and (3), it was assumed that $C_{1g} = C_{2g}$, $L_{11} = L_{22}$, and $M_{1g} = M_{2g}$ since the two coupled lines are balanced.

The phase velocity of the signal on the line is:

$$v_{SE} = \frac{1}{\sqrt{L_{SE}C_{SE}}} = \frac{1}{\sqrt{(L_{11} + L_{gg} - 2M_{1g}) \left(C_{1g} + \frac{C_{12}C_{1g}}{C_{12} + C_{1g}} \right)}} \quad (3)$$

2.1.2 Odd-Mode Operation

Any voltage scheme can be applied to a coupled line system. A signal that transitions from 0 V to 1 V can be launched on one line while the second line is quiet, or vice-versa. It is also possible to launch a similar signal of opposite polarity (0 V to -1 V) on either of the lines while keeping the other line quiet. In the case of *odd-mode operation*, one of the lines is driven with a positive-going voltage while the other line is driven simultaneously with a negative-going voltage. This is also referred to as driving the lines differentially. In the following sub-sections the odd-mode line parameters are derived.

From Figure 1(b), the odd-mode impedances, Z_{OM1} and Z_{OM2} , are:

$$Z_{OM} = Z_{OM1} = Z_{OM2} = \frac{Z_A}{2} \parallel Z_B = \frac{Z_A Z_B}{Z_A + 2Z_B} \quad (4)$$

The characteristic odd-mode impedance is:

$$Z_{OM} = \sqrt{\frac{L_{11} - M_{12}}{C_{1g} + 2C_{12}}} \quad (5)$$

Note that in equation (5), it was assumed that $C_{1g} = C_{2g}$, $L_{11} = L_{22}$, and $M_{1g} = M_{2g}$ since the two coupled lines are balanced. Equation (5) is in agreement with results reported in [8].

The phase velocity of the signal on such a line is:

$$v_{OM} = \frac{1}{\sqrt{L_{OM}C_{OM}}} = \frac{1}{\sqrt{(L_{11} - M_{12})(C_{1g} + 2C_{12})}} \quad (6)$$

2.1.3 Even-Mode Operation

Even-mode operation occurs when both lines of a coupled pair are driven with the same voltage (polarity and amplitude). In the following sub-sections the even-mode line parameters are derived.

From Figure 1(b), the even-mode impedances, Z_{EM1} and Z_{EM2} , are:

$$Z_{EM1} = Z_{EM2} = Z_B \quad (7)$$

The characteristic even-mode impedance is:

$$Z_{EM} = \sqrt{\frac{L_{11} + M_{12} + 2L_{gg} - 4M_{1g}}{C_{1g}}} \quad (8)$$

Note that in equation (8), it was assumed that $C_{1g} = C_{2g}$, $L_{11} = L_{22}$, and $M_{1g} = M_{2g}$ since the two coupled lines are balanced.

The phase velocity of the signal on such a line is:

$$v_{EM} = \frac{1}{\sqrt{L_{EM}C_{EM}}} = \frac{1}{\sqrt{(L_{11} + M_{12} + 2L_{gg} - 4M_{1g})(C_{1g})}} \quad (9)$$

2.1.4 Differential-Mode Operation

In the differential signaling methodology, two signal conductors are used to transmit a single bit of information from the transmitter to the receiver [1]. The lines are placed close to each other in order to achieve coupling between them. Data is transmitted on the two signal conductors in tandem. As one line goes low relative to ground, the other line goes high and vice versa.

From Figures 1(b), the differential-mode impedance, Z_{diff} , is:

$$Z_{diff} = Z_A \parallel 2Z_B = \frac{2Z_A Z_B}{Z_A + 2Z_B} \quad (10)$$

The characteristic differential-mode impedance is:

$$Z_{diff} = \sqrt{\frac{2(L_{11} - M_{12})}{C_{12} + \frac{C_{1g}}{2}}} \quad (11)$$

The phase velocity, v_{diff} , of the signal on such a differential line is:

$$v_{diff} = \frac{1}{\sqrt{L_{diff}C_{diff}}} = \frac{1}{\sqrt{2(L_{11} - M_{12})\left(C_{12} + \frac{C_{1g}}{2}\right)}} \quad (12)$$

2.1.5 Common-Mode Operation

Common-mode operation is usually an undesirable phenomenon because it tends to lead to EMI problems. As a result, there are not many known applications which use common mode. Nonetheless, it exists and hence needs to be characterized. Like differential mode, common mode requires two signal

conductors. A basic difference between the two modes is that in common mode, both signal lines go high or low together.

From Figure 1(b), the common-mode impedance, Z_{CM} , is:

$$Z_{CM} = Z_B \parallel Z_B = \frac{Z_B}{2} \quad (13)$$

The characteristic differential-mode impedance is:

$$Z_{CM} = \sqrt{\frac{(L_{11} + M_{12} + 2L_{gg} - 4M_{1g})}{4C_{1g}}} \quad (14)$$

The phase velocity, v_{CM} , of the signal on such a line is defined as:

$$v_{CM} = \frac{1}{\sqrt{L_{CM}C_{CM}}} = \frac{1}{\sqrt{(L_{11} + M_{12} + 2L_{gg} - 4M_{1g})(C_{1g})}} \quad (15)$$

The impedances and phase velocities of all of the above-mentioned modes are directly or indirectly measurable quantities. After making the measurements, it is subsequently possible to compute the values of the constituent components comprising the coupled-line model, (i.e. Z_A , Z_B , C_{1g} , etc.) The fact that the lines are balanced significantly simplifies this computation as it has the effect of reducing the number of variables for which to solve, and consequently, the number of required measurements. It is possible to calculate both Z_A and Z_B after measuring only the even- and odd-mode impedances. Such a technique is implemented in the coupled-line model in commercial software packages such as TDA Systems IConnect [1].

3. Definition and Theory of Unbalanced Lines

In all the previous discussions, the coupled lines have been assumed to be balanced, both geometrically and temporally. In reality, most practical differential transmission lines have some degree of imbalance. This imbalance can arise due to multiple factors and is sometimes inherent in the design. Even when imbalance is inherent, the measurement method often assumes that the lines are balanced. Simple examples of unbalanced lines include coupled traces on a PCB, which, though meant to be “identical,” might have some differences in geometry. Temporal imbalance also appears in connectors when one of the differential signal pins of the connector is longer than the other. This is referred to as skew. Up to about 1 Gbits/s, imbalances in the system do not impact the performance significantly. With data rates pushing beyond 5 Gbits/s, it becomes important to characterize and understand imbalances. Only by properly characterizing imbalances will it be possible to identify its causes and possibly eliminate it. Similar to balanced coupled transmission lines, there are multiple modes of operation of an unbalanced coupled transmission line. Presented here is the characterization of these modes in terms of their impedance, phase velocity, inductance, and capacitance. The terms inductance and capacitance, wherever used hereon in this chapter shall refer to the per unit length inductance and the per unit length capacitance respectively.

The derivation of the various parameters is presented here for the single-ended operation of unbalanced lines. The parameters for all other modes can be derived in a similar manner and therefore only the final results are presented.

3.1 Unbalanced Single-Ended Operation

Single-ended operation was described earlier in section 2.1.1. In the following sub-sections, the parameters governing the operation of the single-ended mode for unbalanced lines are derived.

3.1.1 Impedance

The single-ended impedance of unbalanced lines can be defined in a similar manner to that of balanced lines, with one prominent difference. For unbalanced lines, the impedance of each signal line to ground is not equal.

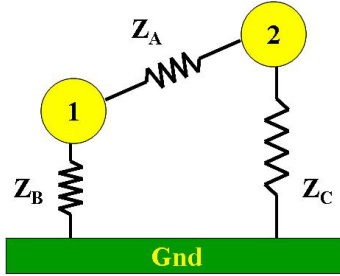


Figure 2: Model of Unbalanced Coupled Lines

From Figure 2, the two single-ended impedances, Z_{SE1} and Z_{SE2} , are:

$$Z_{SE1} = Z_B \parallel (Z_A + Z_C) = \frac{Z_B(Z_A + Z_C)}{Z_A + Z_B + Z_C} \quad (16)$$

$$Z_{SE2} = Z_C \parallel (Z_A + Z_B) = \frac{Z_C(Z_A + Z_B)}{Z_A + Z_B + Z_C} \quad (17)$$

where Z_B and Z_C are the impedance between conductor 1 and ground, and conductor 2 and ground respectively and Z_A is the impedance between conductors 1 and 2.

3.1.2 Capacitance Per Unit Length

The capacitance of each of the single-ended lines in a coupled pair, as shown in Figure 3, is defined as the capacitance of the line to ground taking into account all paths to ground.

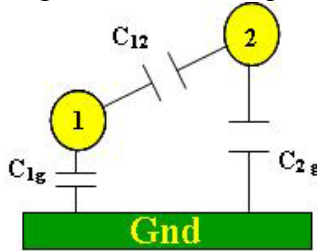


Figure 3: Model Used to Compute Unbalanced Single-Ended Capacitance

The single-ended capacitances, C_{SE1} and C_{SE2} are defined as:

$$C_{SE1} = C_{1g} + \frac{C_{12}C_{2g}}{C_{12} + C_{2g}} \quad (18)$$

$$C_{SE2} = C_{2g} + \frac{C_{12}C_{1g}}{C_{12} + C_{1g}} \quad (19)$$

where C_{12} is the capacitance from conductor 1 to conductor 2, C_{1g} is the capacitance between conductor 1 and ground, and C_{2g} is the capacitance between conductor 2 and ground. Unlike the balanced case

where $C_{1g} = C_{2g}$, for an unbalanced system such as the one shown in Figure 3, $C_{1g} \neq C_{2g}$, and hence $C_{SE1} \neq C_{SE2}$.

3.1.3 Inductance Per Unit Length

The circuit used to calculate the single-ended inductance can be represented as shown in Figure 4. Each conductor, including the ground, has both partial self inductance and partial mutual inductance to other conductors.

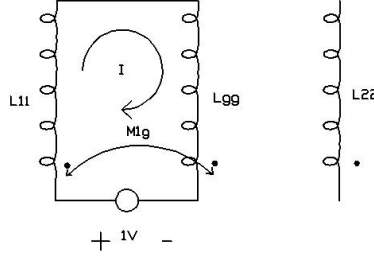


Figure 4: Circuit Used for Computing Unbalanced Single-Ended Inductance

Solving the mesh equation for the loop shown in Figure 4 yields,

$$-1 + j\omega L_{11} + j\omega L_{gg} - j\omega M_{1g} - j\omega M_{1g} = 0, \quad (20)$$

where L_{11} is the partial self inductance of line 1, L_{22} is the partial self inductance of line 2, L_{gg} is the partial self inductance of the ground, and M_{1g} is the partial mutual inductance between line 1 and ground.

This can be reduced to give

$$-1 + j\omega(L_{11} + L_{gg} - 2M_{1g}) = 0, \text{ or} \quad (21)$$

$$-1 + j\omega(L_{SE1}) = 0, \quad (22)$$

where,

$$L_{SE1} = L_{11} + L_{gg} - 2M_{1g}. \quad (23)$$

A similar analysis for L_{SE2} yields

$$L_{SE2} = L_{22} + L_{gg} - 2M_{2g} \quad (24)$$

L_{SE1} is the single-ended loop inductance of line 1, and L_{SE2} is the single-ended loop inductance of line 2. It should be noted that unlike in the case of balanced lines, $L_{11} \neq L_{22}$ and $M_{1g} \neq M_{2g}$, and as a result $L_{SE1} \neq L_{SE2}$.

3.1.4 Characteristic Impedance and Phase Velocity

The characteristic single-ended impedance can be written as:

$$Z_{SE} = \sqrt{\frac{L_{SE}}{C_{SE}}} \quad (25)$$

From equations (18), (19), (23), and (24),

$$Z_{SE1} = \sqrt{\frac{L_{11} + L_{gg} - 2M_{1g}}{C_{1g} + \frac{C_{12}C_{2g}}{C_{12} + C_{2g}}}} \quad (26)$$

$$Z_{SE2} = \sqrt{\frac{L_{22} + L_{gg} - 2M_{2g}}{C_{2g} + \frac{C_{12}C_{1g}}{C_{12} + C_{2g}}}} \quad (27)$$

The phase velocity of the signal on such a line is defined as:

$$v_{SE1} = \frac{1}{\sqrt{L_{SE1}C_{SE1}}} = \frac{1}{\sqrt{(L_{11} + L_{gg} - 2M_{1g}) \left(C_{1g} + \frac{C_{12}C_{2g}}{C_{12} + C_{2g}} \right)}} \quad (28)$$

$$v_{SE2} = \frac{1}{\sqrt{L_{SE2}C_{SE2}}} = \frac{1}{\sqrt{(L_{22} + L_{gg} - 2M_{2g}) \left(C_{2g} + \frac{C_{12}C_{1g}}{C_{12} + C_{2g}} \right)}} \quad (29)$$

3.2 Unbalanced π -Mode Operation

The π -mode operation is similar to the odd-mode operation of balanced lines where the two lines are driven with equal and opposite voltages and corresponding equal and opposite currents. In contrast to the single odd mode of balanced lines, there are two π -modes when the lines are unbalanced. In the following sub-sections, the parameters governing the operation of the π -mode for unbalanced lines are presented.

3.2.1 Impedance

The two π -mode impedances for unbalanced lines are defined as the impedance between either of the lines and ground when the lines are driven differentially. For balanced lines, the impedance was the same irrespective of which line was considered. In the case of unbalanced lines, the π -mode impedance evaluates to two different values depending on which signal conductor is under consideration. In the special case of balanced lines, the two π -mode impedances are equal and become the odd-mode impedance. The two π -mode impedances for unbalanced lines can be defined as follows. From the definition of π -mode impedance, the two π -mode impedances, $Z_{\pi1}$ and $Z_{\pi2}$ are:

$$Z_{\pi1} = \frac{Z_A}{2} \parallel Z_B = \frac{Z_A Z_B}{Z_A + 2Z_B} \quad (30)$$

$$Z_{\pi2} = \frac{Z_A}{2} \parallel Z_C = \frac{Z_A Z_C}{Z_A + 2Z_C} \quad (31)$$

3.2.2 Capacitance Per Unit Length

The π -mode capacitance is defined as the capacitance to ground of either of the lines when the lines are driven differentially. From the definition of π -mode capacitance, the two π -mode capacitances, $C_{\pi1}$ and $C_{\pi2}$ are,

$$C_{\pi 1} = C_{1g} \parallel 2C_{12} = C_{1g} + 2C_{12} \quad (32)$$

$$C_{\pi 2} = C_{2g} \parallel 2C_{12} = C_{2g} + 2C_{12} \quad (33)$$

Note that for an asymmetric lossless coupled line, $C_{1g} \neq C_{2g}$ unlike in the balanced case.

3.2.3 Inductance Per Unit Length

For an asymmetric lossless coupled line, the π -mode inductances can be obtained using mesh analysis.

Unlike in the case of balanced lines, $L_{11} \neq L_{22}$, and $M_{1g} \neq M_{2g}$. The two π -mode inductances, $L_{\pi 1}$ and $L_{\pi 2}$ are:

$$L_{\pi 1} = \left(\frac{L_{11}L_{22} + L_{11}L_{gg} + L_{22}L_{gg} - 2L_{gg}M_{12} - M_{12}^2 - 2L_{22}M_{1g} + 2M_{12}M_{1g} - M_{1g}^2 - 2L_{11}M_{2g} + 2M_{12}M_{2g} + 2M_{1g}M_{2g} - M_{2g}^2}{-L_{22} - 2L_{gg} - M_{12} + M_{1g} + 3M_{2g}} \right) \quad (34)$$

and

$$L_{\pi 2} = \left(\frac{-L_{22}L_{gg} + 2L_{gg}M_{12} + M_{12}^2 + 2L_{22}M_{1g} - 2M_{12}M_{1g} + M_{1g}^2 - L_{11}(L_{22} + L_{gg} - 2M_{2g}) - 2M_{12}M_{2g} - 2M_{1g}M_{2g} + M_{2g}^2}{L_{11} + 2L_{gg} + M_{12} - 3M_{1g} - M_{2g}} \right) \quad (35)$$

3.2.4 Characteristic Impedance and Phase Velocity

Using the values of inductance and capacitance obtained in sections 3.2.2 and 3.2.3, the two characteristic π -mode impedances can also be written as:

$$Z_{\pi 1} = \sqrt{\frac{L_{\pi 1}}{C_{\pi 1}}} \quad (36)$$

Using equations (32), (33), (34) and (35) in (36), yields

$$Z_{\pi 1} = \sqrt{\frac{L_{11}L_{22} + L_{11}L_{gg} + L_{22}L_{gg} - 2L_{gg}M_{12} - M_{12}^2 - 2L_{22}M_{1g} + 2M_{12}M_{1g} - M_{1g}^2 - 2L_{11}M_{2g} + 2M_{12}M_{2g} + 2M_{1g}M_{2g} - M_{2g}^2}{(-L_{22} - 2L_{gg} - M_{12} + M_{1g} + 3M_{2g})(C_{1g} + 2C_{12})}} \quad (37)$$

and

$$Z_{\pi 2} = \sqrt{\frac{-L_{22}L_{gg} + 2L_{gg}M_{12} + M_{12}^2 + 2L_{22}M_{1g} - 2M_{12}M_{1g} + M_{1g}^2 - L_{11}(L_{22} + L_{gg} - 2M_{2g}) - 2M_{12}M_{2g} - 2M_{1g}M_{2g} + M_{2g}^2}{(L_{11} + 2L_{gg} + M_{12} - 3M_{1g} - M_{2g})(C_{2g} + 2C_{12})}} \quad (38)$$

The phase velocity of the signal on such a line is defined as:

$$v_{\pi 1} = \frac{1}{\sqrt{L_{\pi 1}C_{\pi 1}}} = \quad (39)$$

$$\frac{1}{\sqrt{\left(\frac{L_{11}L_{22} + L_{11}L_{gg} + L_{22}L_{gg} - 2L_{gg}M_{12} - M_{12}^2 - 2L_{22}M_{1g} + 2M_{12}M_{1g} - M_{1g}^2 - 2L_{11}M_{2g} + 2M_{12}M_{2g} + 2M_{1g}M_{2g} - M_{2g}^2}{-L_{22} - 2L_{gg} - M_{12} + M_{1g} + 3M_{2g}} \right) (C_{1g} + 2C_{12})}}$$

and

$$v_{\pi 2} = \frac{1}{\sqrt{L_{\pi 2}C_{\pi 2}}} = \quad (40)$$

$$\frac{1}{\sqrt{\left(\frac{-L_{22}L_{gg} + 2L_{gg}M_{12} + M_{12}^2 + 2L_{22}M_{1g} - 2M_{12}M_{1g} + M_{1g}^2 - L_{11}(L_{22} + L_{gg} - 2M_{2g}) - 2M_{12}M_{2g} - 2M_{1g}M_{2g} + M_{2g}^2}{L_{11} + 2L_{gg} + M_{12} - 3M_{1g} - M_{2g}} \right) (C_{2g} + 2C_{12})}}$$

3.3 Unbalanced c-Mode Operation

The c -mode operation, is similar to the even-mode operation of balanced lines where the two lines are driven with equal voltages and corresponding equal currents. In contrast to the single even mode of balanced lines, there are two c -modes when the lines are unbalanced. In the following sub-sections, the parameters governing the operation of the c -mode for unbalanced lines are shown.

3.3.1 Impedance

Similar to the balanced-line case, the two c -mode impedances of unbalanced lines are defined as the impedance between either of the signal lines and ground when they are driven with the same voltage. There are again two c -mode impedances depending on which one of the two lines is under consideration. For the balanced line case, the two c -mode impedances are equal and are called the even-mode impedance.

The two c -mode impedances, Z_{c1} and Z_{c2} , are defined as:

$$Z_{c1} = Z_B \quad (41)$$

$$Z_{c2} = Z_C \quad (42)$$

3.3.2 Capacitance Per Unit Length

The c -mode capacitance is defined as the impedance to ground of either of the transmission lines when they are driven with the same voltage.

The two c -mode capacitance, C_{c1} and C_{c2} , are

$$C_{c1} = C_{1g} \quad (43)$$

$$C_{c2} = C_{2g} \quad (44)$$

Note that for an asymmetric lossless coupled line, $C_{1g} \neq C_{2g}$.

3.3.3 Inductance Per Unit Length

For an unbalanced system, $L_{11} \neq L_{22}$ and $M_{1g} \neq M_{2g}$. The effective inductances, as obtained using mesh analysis on such a circuit are the c -mode inductances, i.e.

$$L_{c1} = \left(\frac{-L_{22}L_{gg} + 2L_{gg}M_{12} + M_{12}^2 + 2L_{22}M_{1g} - 2M_{12}M_{1g} + M_{1g}^2 - L_{11}(L_{22} + L_{gg} - 2M_{2g}) - 2M_{12}M_{2g} - 2M_{1g}M_{2g} + M_{2g}^2}{L_{22} - M_{12} + M_{1g} - M_{2g}} \right) \quad (45)$$

and

$$L_{c2} = \left(\frac{-L_{22}L_{gg} + 2L_{gg}M_{12} + M_{12}^2 + 2L_{22}M_{1g} - 2M_{12}M_{1g} + M_{1g}^2 - L_{11}(L_{22} + L_{gg} - 2M_{2g}) - 2M_{12}M_{2g} - 2M_{1g}M_{2g} + M_{2g}^2}{L_{11} - M_{12} - M_{1g} + M_{2g}} \right) \quad (46)$$

3.3.4 Characteristic Impedance and Phase Velocity

Using the values of inductance and capacitance obtained in sections 3.3.2 and 3.3.3, the two characteristic c -mode impedances can be written as:

$$Z_{c1} = \sqrt{\frac{L_{c1}}{C_{c1}}} \quad (47)$$

Using (43), (44), (45) and (46) in (47), the characteristic c -mode impedances, Z_{c1} and Z_{c2} , can be written as:

$$Z_{c1} = \sqrt{\frac{-L_{22}L_{gg} + 2L_{gg}M_{12} + M_{12}^2 + 2L_{22}M_{1g} - 2M_{12}M_{1g} + M_{1g}^2 - L_{11}(L_{22} + L_{gg} - 2M_{2g}) - 2M_{12}M_{2g} - 2M_{1g}M_{2g} + M_{2g}^2}{(L_{22} - M_{12} + M_{1g} - M_{2g})C_{1g}}} \quad (48)$$

and

$$Z_{c2} = \sqrt{\frac{-L_{22}L_{gg} + 2L_{gg}M_{12} + M_{12}^2 + 2L_{22}M_{1g} - 2M_{12}M_{1g} + M_{1g}^2 - L_{11}(L_{22} + L_{gg} - 2M_{2g}) - 2M_{12}M_{2g} - 2M_{1g}M_{2g} + M_{2g}^2}{(L_{11} - M_{12} - M_{1g} + M_{2g})C_{2g}}} \quad (49)$$

The phase velocity of the signal on such a line is defined as:

$$v_{c1} = \frac{1}{\sqrt{L_{c1}C_{c1}}} = \quad (50)$$

$$\frac{1}{\sqrt{\frac{-L_{22}L_{gg} + 2L_{gg}M_{12} + M_{12}^2 + 2L_{22}M_{1g} - 2M_{12}M_{1g} + M_{1g}^2 - L_{11}(L_{22} + L_{gg} - 2M_{2g}) - 2M_{12}M_{2g} - 2M_{1g}M_{2g} + M_{2g}^2}{(L_{22} - M_{12} + M_{1g} - M_{2g})} (C_{1g})}}$$

and

$$v_{c2} = \frac{1}{\sqrt{L_{c2}C_{c2}}} = \quad (51)$$

$$\frac{1}{\sqrt{\frac{-L_{22}L_{gg} + 2L_{gg}M_{12} + M_{12}^2 + 2L_{22}M_{1g} - 2M_{12}M_{1g} + M_{1g}^2 - L_{11}(L_{22} + L_{gg} - 2M_{2g}) - 2M_{12}M_{2g} - 2M_{1g}M_{2g} + M_{2g}^2}{(L_{22} - M_{12} + M_{1g} - M_{2g})} (C_{2g})}}$$

3.4 Unbalanced Differential-Mode Operation

The differential-mode operation in unbalanced lines is similar to the differential-mode operation of balanced lines. As was stated in section 2.4, in differential-mode operation, as one line goes low relative to ground, the other line goes high and vice versa. In the following sub-sections, the parameters governing the operation of the differential-mode for unbalanced lines are derived.

3.4.1 Impedance

Since differential impedance is defined as the impedance measured between the two conductors, it can be obtained for the unbalanced line case in a similar manner to the balanced line case. The differential impedance, Z_{diff} is:

$$Z_{diff} = Z_A \parallel (Z_B + Z_C) = \frac{Z_A(Z_B + Z_C)}{Z_A + Z_B + Z_C} \quad (52)$$

3.4.2 Capacitance Per Unit Length

The differential-mode capacitance is defined as the effective capacitance between two signal conductors. The differential-mode capacitance, C_{diff} , is:

$$C_{diff} = C_{12} \parallel \left(\frac{C_{1g}C_{2g}}{C_{1g} + C_{2g}} \right) = C_{12} + \left(\frac{C_{1g}C_{2g}}{C_{1g} + C_{2g}} \right) \quad (53)$$

Note that in (63), $C_{1g} \neq C_{2g}$, unlike in the case of balanced lines.

3.4.3 Inductance Per Unit Length

The differential-mode inductance of a balanced system is simply the sum of the two odd-mode inductances. However, for the case of the unbalanced line, the differential-mode inductance is something very different.

Solving for L_{diff} yields

$$L_{diff} = (L_{11} + L_{22} - 2M_{12}) \quad (54)$$

3.4.4 Characteristic Impedance and Phase Velocity

The characteristic differential impedance can be written as:

$$Z_{diff} = \sqrt{\frac{L_{diff}}{C_{diff}}} \quad (55)$$

From (53), and (54),

$$Z_{diff} = \sqrt{\frac{(L_{11} + L_{22} - 2M_{12})}{C_{12} + \left(\frac{C_{1g}C_{2g}}{C_{1g} + C_{2g}}\right)}} \quad (56)$$

It should be noted that in the case of unbalanced lines, $Z_{OM} \neq \frac{Z_{diff}}{2}$.

The phase velocity of the signal on such a line is defined as:

$$v_{diff} = \frac{1}{\sqrt{L_{diff}C_{diff}}} = \frac{1}{\sqrt{(L_{11} + L_{22} - 2M_{12}) \left(C_{12} + \left(\frac{C_{1g}C_{2g}}{C_{1g} + C_{2g}} \right) \right)}} \quad (57)$$

3.5 Unbalanced Common-Mode Operation

The common-mode operation in unbalanced lines is similar to the common-mode operation of balanced lines. As was stated in section 2.5, common-mode operation is not something which is very desirable but since it still exists, it needs to be characterized. In common-mode operation, both signal lines go high or low together. This implies that the two signal lines are effectively shorted together. In the following subsections, the parameters governing the operation of the common-mode for unbalanced lines are derived.

3.5.1 Impedance

The common-mode impedance for the unbalanced-line case is the impedance between the two signal lines and the ground when the two signal lines are shorted together. The unbalanced line common-mode impedance, Z_{CM} , can be obtained as:

$$Z_{CM} = Z_B \parallel Z_C = \frac{Z_B Z_C}{Z_B + Z_C} \quad (58)$$

It should be noted that unlike in the balanced line case, $Z_{EM} \neq 2Z_{CM}$.

3.5.2 Capacitance Per Unit Length

The common-mode capacitance is defined as the effective capacitance from the pair of shorted signal lines to ground. The common-mode capacitance, C_{CM} , is:

$$C_{CM} = C_{1g} \parallel C_{2g} = C_{1g} + C_{2g} \quad (59)$$

3.5.3 Inductance Per Unit Length

As does differential-mode operation, common-mode operation also requires two signal lines. In contrast to differential mode, in common mode, both lines go high or low together. This amounts to the shorting of the two signal lines. For an unbalanced system, $L_{11} \neq L_{22}$ and $M_{1g} \neq M_{2g}$. The common-mode inductance is:

$$L_{CM} = \left(-\frac{-L_{22}L_{gg} + 2L_{gg}M_{12} + M_{12}^2 + 2L_{22}M_{1g} - 2M_{12}M_{1g} + M_{1g}^2 - L_{11}(L_{22} + L_{gg} - 2M_{2g}) - 2M_{12}M_{2g} - 2M_{1g}M_{2g} + M_{2g}^2}{L_{11} + L_{22} - 2M_{12}} \right) \quad (60)$$

3.5.4 Characteristic Impedance and Phase Velocity

The characteristic common-mode impedance can be written as:

$$Z_{CM} = \sqrt{\frac{L_{CM}}{C_{CM}}} \quad (61)$$

From equations (59), and (60),

$$Z_{CM} = \sqrt{\frac{-L_{22}L_{gg} + 2L_{gg}M_{12} + M_{12}^2 + 2L_{22}M_{1g} - 2M_{12}M_{1g} + M_{1g}^2 - L_{11}(L_{22} + L_{gg} - 2M_{2g}) - 2M_{12}M_{2g} - 2M_{1g}M_{2g} + M_{2g}^2}{(L_{11} + L_{22} - 2M_{12})(C_{1g} + C_{2g})}} \quad (62)$$

The phase velocity of a common-mode signal on such a line is defined as:

$$v_{CM} = \frac{1}{\sqrt{L_{CM}C_{CM}}} = \quad (63)$$

$$\frac{1}{\sqrt{\frac{-L_{22}L_{gg} + 2L_{gg}M_{12} + M_{12}^2 + 2L_{22}M_{1g} - 2M_{12}M_{1g} + M_{1g}^2 - L_{11}(L_{22} + L_{gg} - 2M_{2g}) - 2M_{12}M_{2g} - 2M_{1g}M_{2g} + M_{2g}^2}{(L_{11} + L_{22} - 2M_{12})(C_{1g} + C_{2g})}}}$$

As in the case of balanced lines, the above-mentioned impedances and phase velocities of all of the modes are directly or indirectly measurable. However, when the lines are unbalanced, it becomes much more difficult to compute the constituent components comprising the coupled-line model. A minimum of three measurements is now required, as opposed to the two needed for the balanced case. Three fairly easily obtained measurements include the two single-ended impedances Z_{SE1} , Z_{SE2} , and the differential impedance Z_{diff} .

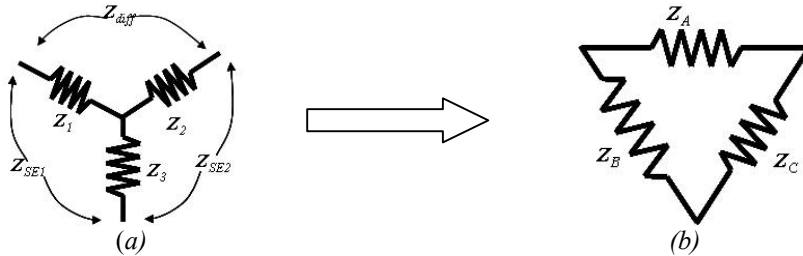


Figure 5: (a) "Wye" configuration. (b) Delta configuration.

The single-ended and differential impedances can be placed into a "wye" interconnection as shown in Figure 5(a), and represented in terms of Z_1 , Z_2 , and Z_3 , as:

$$\begin{aligned} Z_1 + Z_2 &= Z_{diff} \\ Z_1 + Z_3 &= Z_{SE1} \\ Z_2 + Z_3 &= Z_{SE2} \end{aligned} \quad (64)$$

A simple “wye”-to-“delta” transformation as shown in Figure 5(b) yields the values of the constituent components Z_A , Z_B , and Z_C , as:

$$\begin{aligned} Z_A &= -\frac{Z_{SE1}^2 + (Z_{SE2} - Z_{diff})^2 - 2Z_{SE1}(Z_{SE2} + Z_{diff})}{2(Z_{SE1} + Z_{SE2} - Z_{diff})} \\ Z_B &= \frac{Z_{SE1}^2 + (Z_{SE2} - Z_{diff})^2 - 2Z_{SE1}(Z_{SE2} + Z_{diff})}{2(Z_{SE1} - Z_{SE2} - Z_{diff})} \\ Z_C &= -\frac{Z_{SE1}^2 + (Z_{SE2} - Z_{diff})^2 - 2Z_{SE1}(Z_{SE2} + Z_{diff})}{2(Z_{SE1} - Z_{SE2} + Z_{diff})} \end{aligned} \quad (65)$$

A similar approach can be taken to obtain the constituent capacitances C_{I2} , C_{Ig} , and C_{2g} , as shown in Figure 3. Computing the constituent partial self- and mutual-inductances is a cumbersome process beyond the scope of this paper.

The above-described general model of unbalanced lines applies regardless of whether the imbalance is geometrical in nature or the result of in-pair skew. One example of coupled lines with skew is a right-angle connector. Such a structure can be notoriously difficult if not impossible to model by using a balanced coupled-line model. In the balanced case, it is only necessary to measure the impedances and phase velocities of two modes such as the even- and odd-mode, in order to obtain a complete description of the lines. By contrast, in lines possessing in-pair skew, not only would there be two possibly different odd-mode impedances, but the electrical lengths traversed by the two odd-modes would be different.

4. Analysis of Unbalanced Coupled Line Structures

In section 3, the theory of the different modes of propagation and operation of unbalanced lines was derived in terms of their characteristic impedances and phase velocities. Presented next is a mathematical analysis of two example unbalanced structures, one with in-pair skew, and one with geometrical imbalance. The line with skew is also analyzed in terms of S-parameters. The analysis is compared with measurements taken on these unbalanced structures using a vector network analyzer (VNA) and a time-domain reflectometer (TDR). In addition, it is ascertained whether or not the TDR and VNA instrumentation operate with the implicit assumption that the structure being measured is balanced.

4.1 Structure with In-Pair Skew

A structure possessing in-pair skew is said to be temporally unbalanced. The two signal lines comprising the pair have different electrical lengths. A simple example of such an unbalanced line is a pair of coaxial cables with one of the cables being longer than the other.

4.1.1 S-Parameters of Temporally Unbalanced Pair

To illustrate the process of obtaining unbalanced mixed-mode S-parameters, consider a pair of coaxial cables with one of the cables being longer than the other as shown in Figure 6. This is a simple example of a differential pair with temporal imbalance (skew). The time taken by a signal to travel through each of the cables is different because the electrical lengths of the two coaxial cables are different. For simplicity, the coaxial cables are assumed to be lossless.

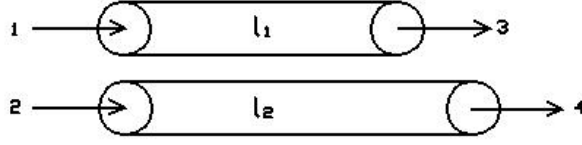


Figure 6: Pair of Unbalanced Coaxial-Cables

The particular coaxial cables used for the purpose of this experiment were the Semi-flex RG405 cables. The center conductor diameter was 0.51 mm while the diameter of the PTFE dielectric was 1.7 mm.

In the case of an ideal lossless coaxial cable, the entire signal is transmitted through to the receiving end. Also, there will be no reflections when the cable is terminated in its characteristic impedance. The single-ended S-parameters for the two cables of lengths l_1 and l_2 can be written as:

$$S_{cable1} = \begin{pmatrix} 0 & e^{-j\beta_1 l_1} \\ e^{-j\beta_1 l_1} & 0 \end{pmatrix}, S_{cable2} = \begin{pmatrix} 0 & e^{-j\beta_2 l_2} \\ e^{-j\beta_2 l_2} & 0 \end{pmatrix} \quad (66a, 66b)$$

When considered as a differential pair, the 4-port single-ended S-parameters of the coaxial cables in Figure 6 can be written as:

$$S_{SE4p} = \begin{pmatrix} S_{cable1}(1,1) & 0 & S_{cable1}(1,2) & 0 \\ 0 & S_{cable2}(1,1) & 0 & S_{cable2}(1,2) \\ S_{cable1}(2,1) & 0 & S_{cable1}(2,2) & 0 \\ 0 & S_{cable2}(2,1) & 0 & S_{cable2}(2,2) \end{pmatrix} \\ = \begin{pmatrix} 0 & 0 & e^{-j\beta_1 l_1} & 0 \\ 0 & 0 & 0 & e^{-j\beta_2 l_2} \\ e^{-j\beta_1 l_1} & 0 & 0 & 0 \\ 0 & e^{-j\beta_2 l_2} & 0 & 0 \end{pmatrix} \quad (67)$$

Note that in (67) all the crosstalk terms are assumed to be zero because, there is no coupling between the two coaxial cables.

The single-ended S-parameters can be converted to mixed mode S-parameters using the transformation in [9]. This gives us:

$$S_{Mixed} = \left(\begin{array}{cc|cc} 0 & \frac{1}{2}(e^{-j\beta_1 l_1} + e^{-j\beta_2 l_2}) & 0 & \frac{1}{2}(e^{-j\beta_1 l_1} - e^{-j\beta_2 l_2}) \\ \frac{1}{2}(e^{-j\beta_1 l_1} + e^{-j\beta_2 l_2}) & 0 & \frac{1}{2}(e^{-j\beta_1 l_1} - e^{-j\beta_2 l_2}) & 0 \\ \hline 0 & \frac{1}{2}(e^{-j\beta_1 l_1} - e^{-j\beta_2 l_2}) & 0 & \frac{1}{2}(e^{-j\beta_1 l_1} + e^{-j\beta_2 l_2}) \\ \frac{1}{2}(e^{-j\beta_1 l_1} - e^{-j\beta_2 l_2}) & 0 & \frac{1}{2}(e^{-j\beta_1 l_1} + e^{-j\beta_2 l_2}) & 0 \end{array} \right) \quad (68)$$

These are the values obtained when using the single-ended to mixed-mode transformations as used by vector network analyzers.

4.1.2 Measurement of Temporally Unbalanced Pair

Measurements were taken on a pair of unbalanced coaxial cables of lengths 0.195 m and 0.288 m using the HP8720ES/ATN-4112A 4-Port Vector Network Analyzer. The launch cable loss was removed from the test data by calibrating the VNA to the end of the launch cables. These measurements were converted to the mixed-mode parameters using the transformations described in [9]. The measurements were then compared to analytical results obtained from the mathematical model previously developed and from the commercially available software, Agilent Eagleware Genesys (henceforth referred to simply as Genesys,) in order to establish the validity of the mathematical model. Presented here are the three sets of data. The first data set was obtained from measurements taken in the lab using the VNA. The second was obtained from equation (68). All calculations for the second set of data were performed in Mathematica, from Wolfram Research. The third data set was obtained using library components taken from the library of the commercially available software, Genesys. Figure 7 shows the magnitude of the insertion loss for each of the three data sets. Figure 8 shows the phase of the same.

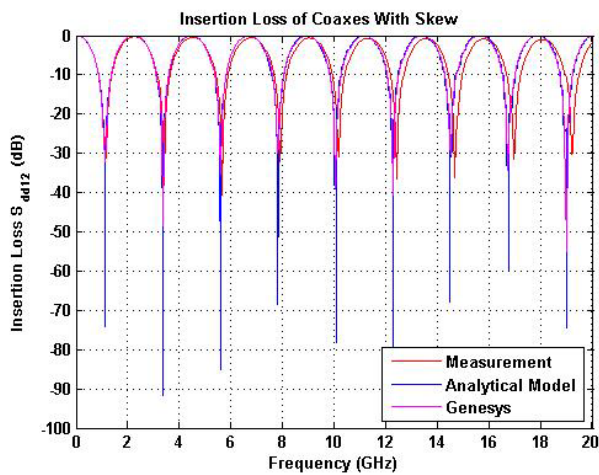


Figure 7: S_{diff}^{12} Magnitude For a Temporally Unbalanced Coaxial Cable Pair.

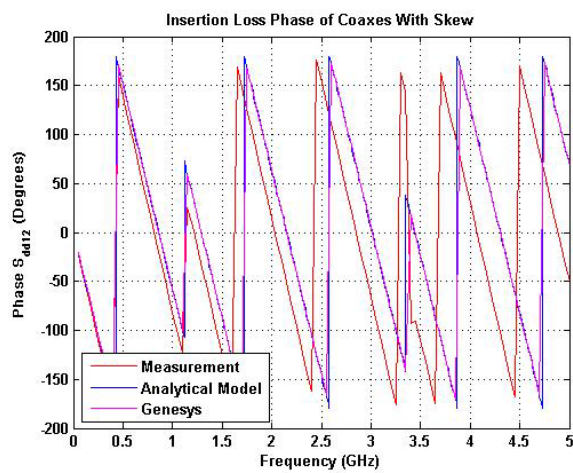


Figure 8: S_{diff}^{12} Phase for a Temporally Unbalanced Coaxial Cable Pair

As can be seen from Figure 7, there is a very good level of correlation between the S-parameters magnitudes as obtained from the three different sources. It is easy to note that there is a difference in the resolution of the insertion loss at the resonant frequencies, as predicted by the analytical model, compared to the measurements using the VNA, and from Genesys. This can be explained by the fact that Mathematica, being an inherently mathematical and high accuracy tool, has a much higher resolution at those already low values (below -30 to -40 dB).

Figure 8 shows that the phase, as obtained from both Genesys and the mathematical model are in good agreement with each other but do not agree with the measured data. To explain the apparent disagreement, it should be noted that the device under test had SMA connectors at the ends of the coaxial cables, and these connectors were not taken into account in either of the models. Measurement of the impedance profile on a TDR indicated that these SMA connectors tended to be inductive in nature. Hence, simple inductances were placed at the ends of the coaxial cables in the Genesys simulations as shown in Figure 9 to ascertain their effects on the phase data. The result of this experiment appears in Figure 10.

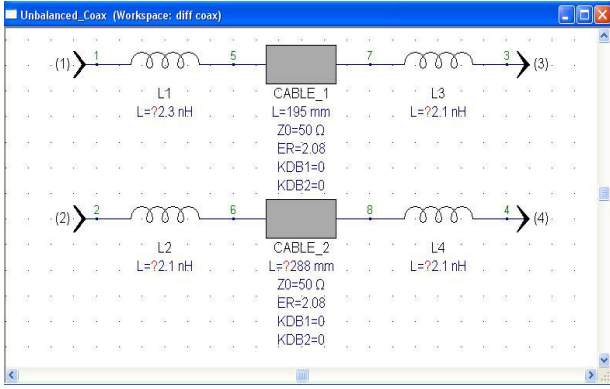


Figure 9: Genesys Model of Unbalanced Coax Cables Including Lumped Inductances to Account for the SMA Connectors on the Ends

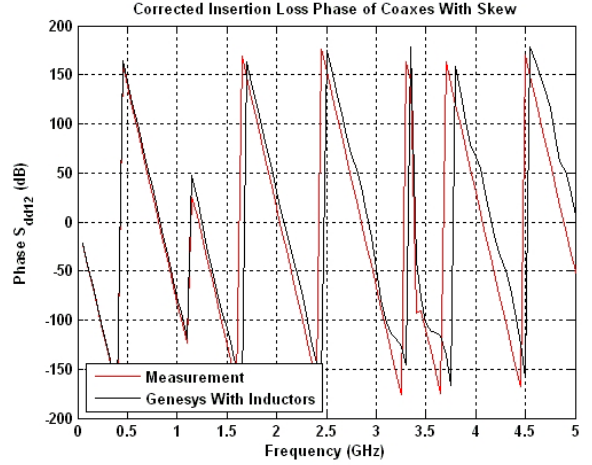


Figure 10: Comparison of the Phase Between the Measured Data and the Genesys Model That Includes Inductors to Account for the SMA Connectors on the Ends

Inclusion of the inductive discontinuities at the beginning and end of the coaxial cables resulted in the Genesys phase data changing to mirror the measurement data. Based on this observation, one can say that the mathematical S-parameter model developed earlier is accurate. Returning now to the various definitions of modal inductance and capacitances for an unbalanced line, it is possible to see which of these are actually measured in the frequency domain when using the VNA with the transformation in [9] or in the time domain when using the TDR.

Let the partial self inductances and capacitances of a pair of unbalanced coaxial cables be L_{11} , L_{22} and C_{1g} , C_{2g} respectively. Because the two cable center conductors are completely shielded from one another, and hence, uncoupled, there are no mutual inductances or mutual capacitances. For this two-conductor system, the differential inductance L_{diff} (as given in equation (64)), is simply the sum of the two inductances while the differential capacitance C_{diff} (as given in equation (63)), is the series combination of the two capacitances. This can be represented as:

$$L_{diff} = L_{11} + L_{22}, \text{ and} \quad (69)$$

$$C_{diff} = \frac{C_{1g}C_{2g}}{C_{1g} + C_{2g}}. \quad (70)$$

The propagation delay of the true differential-mode for the unbalanced coaxial cable can thus be calculated as:

$$t_{pd} = \sqrt{L_{diff}C_{diff}} = \sqrt{\frac{(L_{11} + L_{22})C_{1g}C_{2g}}{C_{1g} + C_{2g}}}. \quad (71)$$

Invoking the equations for the inductance and capacitance of a coaxial cable [10] yields:

$$t_{pd} = \frac{\left(\frac{\mu_1}{2\pi} \ln\left(\frac{d_o}{d_i}\right) l_1 + \frac{\mu_2}{2\pi} \ln\left(\frac{d_o}{d_i}\right) l_2 \right) \left(\frac{2\pi\epsilon_1}{\ln\left(\frac{d_o}{d_i}\right)} l_1 \right) \left(\frac{2\pi\epsilon_2}{\ln\left(\frac{d_o}{d_i}\right)} l_2 \right)}{\left(\frac{2\pi\epsilon_1}{\ln\left(\frac{d_o}{d_i}\right)} l_1 \right) + \left(\frac{2\pi\epsilon_2}{\ln\left(\frac{d_o}{d_i}\right)} l_2 \right)}. \quad (72)$$

Observing that the μ and ϵ values of the two cables are the same, the common terms between the numerator and the denominator cancel out in equation (72) leaving

$$t_{pd} = \sqrt{\mu\epsilon l_1 l_2}. \quad (73)$$

This final form suggests that the effective length of the true differential mode in the case of the unbalanced coaxial cable is the geometric mean of the individual cable lengths, i.e.,

$$l_{eff-diff} = \sqrt{l_1 l_2}. \quad (74)$$

This propagation delay value can be used to construct a simple S-parameter model for the through transmission of a differential-mode signal using an unbalanced coaxial cable pair. The differential-mode transmission would be:

$$S_{diff}^{12} = e^{-j\beta l_{eff-diff}} = e^{-j\beta \sqrt{l_1 l_2}}. \quad (75)$$

On the other hand, the same parameter, as obtained by using the transformations in [9] used by the VNA, is shown in equation (68) as:

$$S_{diff}^{12} = e^{-j\beta l_1} + e^{-j\beta l_2}. \quad (76)$$

This is actually the insertion loss of the sum of the π -modes as opposed that of the true differential mode.

By comparing the three step responses obtained from the VNA and from equation (75) and (76), and plotting them in Figure 11, it is possible to ascertain which insertion loss the VNA actually measures.

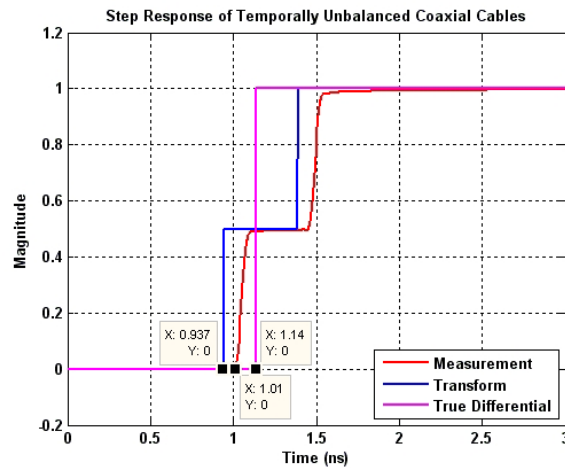


Figure 11: Step Response of S_{diff}^{12} as Obtained From Measurement, Mathematical Model and of True-Differential Mode

From Figure 11, it can be concluded that the differential mode as measured and transformed to the mixed-mode S-parameters [9] by the VNA is actually the insertion loss of the sum of the π -modes and not that of the true differential mode. Hence, the step response of the measurement result agrees with the step response of equation (76).

The difference observed between the time of occurrence of the first step of the measurement (1.01 ns) and that of the equation (76) (0.937 ns,) can be explained by taking note of the fact that the measurement includes two SMA connectors which are about 0.3” long. These SMA connectors have a Teflon core, and the delay through each of these connectors can be calculated as:

$$t_{d-SMA} = \frac{(0.3 \text{ in} * 0.0254 \text{ m/in})}{\left(\frac{3 * 10^8 \text{ m/s}}{\sqrt{2.08}} \right)} \approx 36.63 * 10^{-12} \text{ s} = 36.63 \text{ ps} \quad (77)$$

The total delay through the two SMA connectors is approximately 73.26 ps, which is very close to the difference in time between the measurement data when compared to data obtained from the analytical model which uses (77), the sum of the π -modes. That delay is 73 ps.

4.2 Structure with Geometrical Imbalance

Impedance profiles of coupled microstrip lines are typically measured using a TDR device. As outlined in [11], the differential impedance as measured on a TDR consists of the sum of the odd-modes (π -modes.) This is illustrated in the following example of unbalanced microstrip lines.

4.2.1 Measurement of Geometrically Unbalanced Microstrip Lines

Consider a system of unbalanced microstrip lines above a ground plane, a cross section of which is shown in Figure 12.

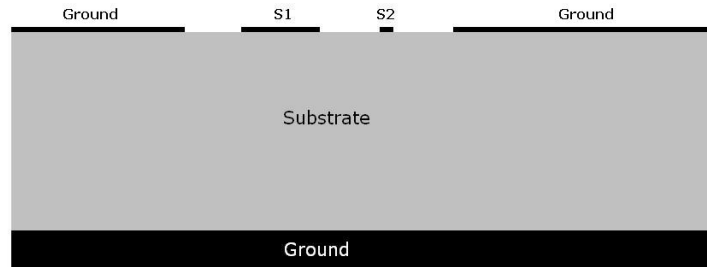


Figure 12: Unbalanced Microstrip Lines Above a Ground Plane

S1 and S2 are two microstrip lines of thickness 1.4 mils and widths of 22.3 mils and 3.7 mils respectively. The distance between the two signal traces, S1 and S2 is 17 mils. S1 is 16 mils from the coplanar ground near it, while S2 is 17 mils away from the coplanar ground near it. The thickness of the substrate is 56.1 mils. These dimensions are taken from a test board which was built specifically in order to study an unbalanced microstrip coupled-line pair. A model of the 2-D cross section of the test board geometry was created and analyzed in Ansoft 2D Parameter Extractor. Capacitance and inductance matrices for the geometry were obtained from the solver. These matrices are:

$$C(\text{farads/m}) = \begin{array}{c|ccc} & \text{Sig 1} & \text{Sig 2} & \text{Gnd} \\ \hline \text{Sig 1} & 6.0654 E-11 & -1.2359 E-11 & -4.8295 E-11 \\ \text{Sig 2} & -1.2359 E-11 & 3.7164 E-11 & -2.4806 E-11 \\ \text{Gnd} & -4.8295 E-11 & -2.4806 E-11 & 7.3101 E-11 \end{array} \quad (78)$$

	Sig 1	Sig 2	Gnd
$L(\text{henry} / \text{m}) =$			
Sig 1	$1.4807 E - 6$	$1.1993 E - 6$	$1.0648 E - 6$
Sig 2	$1.1993 E - 6$	$1.7306 E - 6$	$1.0676 E - 6$
Gnd	$1.0648 E - 6$	$1.0676 E - 6$	$1.0903 E - 6$

(79)

Based on these values of capacitances and inductances, the various impedances and propagation delays for different modes of operation of this transmission line are (using the theory developed in section 3):

$Z_0^{SE1} = 88.3533$	$t_{pd}^{SE1} = 4.99585 \times 10^{-9}$	(Single - ended mode 1)
$Z_0^{SE2} = 140.681$	$t_{pd}^{SE2} = 4.87414 \times 10^{-9}$	(Single - ended mode 2)
$Z_0^{true-diff} = 168.138$	$t_{pd}^{true-diff} = 4.83353 \times 10^{-9}$	(True differential mode)
$Z_0^{cm} = 68.4008$	$t_{pd}^{cm} = 5.00017 \times 10^{-9}$	(Common mode)
$Z_0^{\pi 1} = 67.2048$	$t_{pd}^{\pi 1} = 4.90682 \times 10^{-9}$	(π - mode 1)
$Z_0^{\pi 2} = 96.8304$	$t_{pd}^{\pi 2} = 4.79543 \times 10^{-9}$	(π - mode 2)
$Z_0^{c1} = 104.355$	$t_{pd}^{c1} = 5.03984 \times 10^{-9}$	(c - mode 1)
$Z_0^{c2} = 198.563$	$t_{pd}^{c2} = 4.92555 \times 10^{-9}$	(c - mode 2)
$Z_0^{\pi 1} + Z_0^{\pi 2} = 164.0352$		(Sum of π - modes)

(80)

As can be seen from equation (80), the impedance obtained by summing the two π -mode impedances, 164.0352 ohms, is not equal to the true differential impedance, 168.138 ohms. What remains to be seen now is confirmation that the TDR measures the sum of the π -mode impedances as opposed to the true differential impedance.

The impedance profile obtained by taking measurements on the test board is presented in Figure 13.

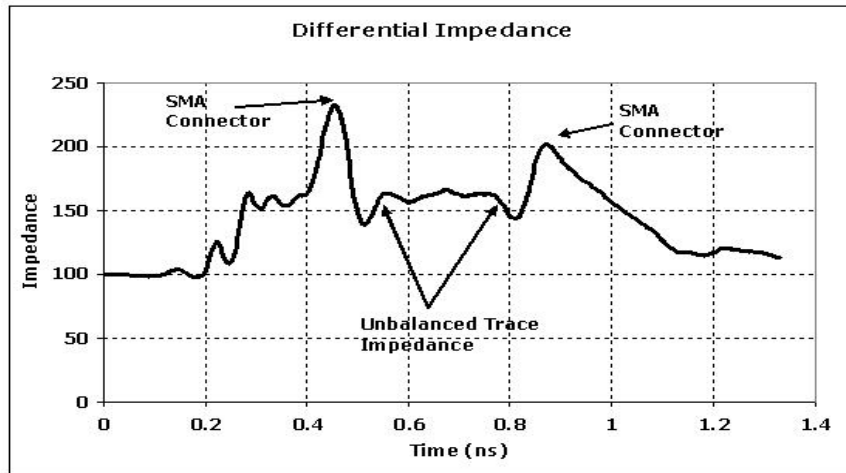


Figure 13: Impedance Profile of Unbalanced Microstrip Structure Measured with TDR

The average impedance over the length of the microstrip traces is close to 164 Ω , located between 0.55 ns and 0.8 ns. This means that the impedance obtained with the TDR is the sum of the π -mode impedances as expected.

5. Conclusions and Future Work

Beginning with the well-known characterization of balanced coupled lines and the termination thereof, this paper extended the theory to present a thorough analysis and model of unbalanced lines. For each of the TEM or quasi-TEM modes of transmission and operation, (single-ended, differential, π -mode, etc.) expressions were given for the impedances and phase velocities in terms of the constituent inductances and capacitances. In addition, a technique was shown for computing the constituent component values given the modal values by making use of a “wye”-to-“delta” transformation. Obtaining the constituent component values can provide a physical understanding of the source of the imbalance within the geometry of the transmission structure, and could possibly be useful in understanding how to eliminate it.

The theoretical model was used to mathematically analyze two unbalanced structures including a pair of coaxial cables with skew and a printed circuit board with geometrically unbalanced microstrip traces. The model results were validated by a comparison with measurements on specially built test structures. Further, the results agreed with those obtained using commercially available software like Agilent Eagleware Genesys, and Ansoft 2D Parameter Extractor.

It should be noted that the differential impedance of an unbalanced line can be defined in two ways. One of the ways is the method described in section 3.4, which is the true differential impedance. The second method is to add the two π -mode impedances. Balanced lines are actually a special case of unbalanced lines. For balanced lines, the two π -mode impedances are equal and are called the odd-mode impedance which is half of the differential impedance. This relationship does not hold for the general case of unbalanced lines.

Despite the desire to use only balanced lines in differential-mode applications, imbalance does occur either in the form of skew or sometimes even geometrically such as in the unsymmetrical location of a drain wire. Given the fact that unbalanced lines exist in many applications, it would be useful to be able to determine how much imbalance is tolerable in a given application. To this end, future work in the characterization of unbalanced lines might consist of defining some sort of figure-of-merit which would define the degree or severity of the imbalance.

6. References

- [1] "Characterization of differential interconnects from TDR measurements," – Application Note, TDA Systems.
- [2] Eric Bogatin, *Signal Integrity - Simplified*. 1st ed., NJ: Prentice Hall PTR, 2004.
- [3] S.B. Cohn, "Shielded Coupled-Strip Transmission Line," *IRE Transactions on Microwave Theory Techniques*, vol. MTT-5, no.10, pp.29-38, Oct. 1955.
- [4] G.I. Zysman, A.K. Johnson, "Coupled Transmission Line Networks in an Inhomogeneous Dielectric Medium," *IEEE Transactions on Microwave Theory and Techniques*, vol. MTT-17, no. 10, Oct. 1969.
- [5] V.K. Tripathi, "Asymmetric coupled transmission lines in an inhomogeneous medium," *IEEE Transactions on Microwave Theory and Techniques*, vol. MTT-23, no. 9, pp. 734-739, Sept. 1975.
- [6] K. Kurokawa, "Power waves and the scattering matrix," *IEEE Transactions on Microwave Theory and Techniques*, vol. MTT-13, no.2, pp. 194-202, Mar. 1965.
- [7] David E. Bockelman, William E. Eisenstadt, "Combined differential- and common-mode scattering parameters: theory and simulation," *IEEE Transactions on Microwave Theory and Techniques*, vol. 43, no. 7, July 1995.
- [8] S.H., Hall, G.W., Hall, J.A., McCall, *High-Speed Digital Design: A Handbook of Interconnect Theory and Design Practices*, John Wiley & Sons, 2000.
- [9] David M. Pozar, *Microwave Engineering*, 3th ed., John Wiley & Sons, 2005.
- [10] Clayton R. Paul, *Analysis of Multiconductor Transmission Lines*, John Wiley & Sons, 1994.
- [11] TDR Impedance Measurements: A Foundation for Signal Integrity, Tektronix Application Note.